J Solid State Electrochem (2001) 5: 531–537
DOI 10.1007/s100080000187

ORIGINAL PAPER

Venkataraman Thangadurai · Robert A. Huggins
Werner Weppner

Mixed ionic-electronic conductivity in phases in the praseodymium oxide system

Received: 12 May 2000 / Accepted: 28 October 2000 / Published online: 13 June 2001

Abstract The praseodymium oxide system contains a series of related phases with very narrow compositional width and unique extended defect structures, rather than the more common isolated point defects. The electrical conductivity of three of these phases has been measured by the use of AC complex impedance and DC methods in the temperature range 75–400 °C. The beta phase, Pr_6O_{11}, exhibits a total conductivity of 6.77×10^{-2} S/cm at 400 °C, with an activation energy of 0.52 eV/atom. The conductivity of the epsilon phase, Pr_5O_9, is slightly lower, with an activation energy of 0.51 eV/atom. The iota phase, Pr_7O_{12}, has a very low conductivity. The activation energies for electrical transport in the beta and epsilon phases are in the general range found in a number of mixed conductors based upon LSGM oxides.

Keywords Praseodymium oxides · Oxide ion conduction · Mixed conduction · Intermediate temperature conductor · Electrical properties

Introduction

Rare earth oxides have been of continuous interest owing to their important electrical, optical and magnetic properties. The praseodymium oxides are particularly intriguing, as they are among the group of binary oxides that show a wide range of stoichiometry, but in which the deviation from the ideal stoichiometry is not continuous, as is expected from the classical model of randomly distributed isolated point defects. Instead, there are a number of phases of unique structures and stoichiometries with no appreciable concentrations of isolated point defects, and thus essentially no compositional width. These structures are closely related to each other, and to a simple "mother" structure. Discussions of this general class of materials have been published [1, 2].

In the case of the praseodymium oxide system, these phases have been shown to have cation sublattices essentially identical to that of fluorite-type PrO_2. The stoichiometric differences between them are accommodated by the presence of topotactically ordered arrangements of large localized concentrations of oxide ion vacancies that divide the structure up into microdomains. There are six sub-oxide phases in addition to the mother phase PrO_2. They form a homologous series whose compositions can be written as Pr_nO_{2n-2}. The compositions of these phases are listed in Table 1. Several investigators have studied the structures and thermodynamic properties of materials in this binary system [3, 4, 5, 6].

The phase diagram of this system, projected onto the temperature-composition plane, is shown in Fig. 1. Because these are oxides, their ranges of equilibrium pressure are different. Thus they cannot all be prepared at an ambient pressure of one atmosphere. The oxygen partial pressure-temperature relationship for the stability of the various phases is shown in Fig. 2. The praseodymium oxide system is unique in that the phase Pr_6O_{11} (or $PrO_{1.83}$), rather than the mother phase PrO_2, is stable at ambient temperatures in air.

Transitions between these phases upon heating and cooling, as well as upon changes in the oxygen activity of their environment, occur very rapidly, indicating unusually high oxygen mobility. This is also indicated by the fact that it was found difficult to cool fast enough to freeze-in equilibrium compositions above about 350–400 °C [3].

Because of the large concentrations of ordered oxygen vacancies in the sub-oxide phases, they can absorb significant amounts of water, even at ambient temperature, apparently by the electrically neutral mechanism proposed by Stotz and Wagner [7, 8]. This involves the

V. Thangadurai · R.A. Huggins (✉) · W. Weppner
Faculty of Engineering, Christian Albrechts University,
24143 Kiel, Germany
E-mail: rhg@techfak.uni-kiel.de
Tel.: +49-0431-880-6212
Fax: +49-0431-880-6203

absorption of oxide ions at sites where there were previously oxide ion vacancies. Protons are also absorbed, and reside in interstitial sites. This water is irreversibly desorbed at relatively low temperatures, indicating high mobility of both protons and either hydroxide ions or oxide ions.

Electrochemical experiments have been employed to study the insertion behavior of lithium into these unusual structures, both with and without the initial presence of protons as the result of the absorption of water [9]. When protons are present, the entry of lithium results in a displacement reaction and the expulsion of hydrogen. Since this does not cause any change in the charge balance, it has no effect upon the oxygen stoichiometry.

Electrochemical experiments are reported here that were undertaken to investigate charge transport in these extended defect structure materials in the temperature range 75–400 °C. By variation of the oxygen partial pressure the samples could be reversibly transformed between the beta and epsilon phases. Prior work [10] primarily involved measurements at higher temperatures, including conditions under which

Table 1 Stoichiometry of the known members of the homologous series Pr_nO_{2n-2}

Value of n	Formula	x in PrO_x	Av. oxidation state of Pr
4	Pr_2O_3	1.500	3.00
7	Pr_7O_{12}	1.714	3.428
9	Pr_9O_{16}	1.778	3.556
10	Pr_5O_9	1.800	3.600
11	$Pr_{11}O_{20}$	1.818	3.636
12	Pr_6O_{11}	1.833	3.667
Infinity	PrO_2	2.000	4

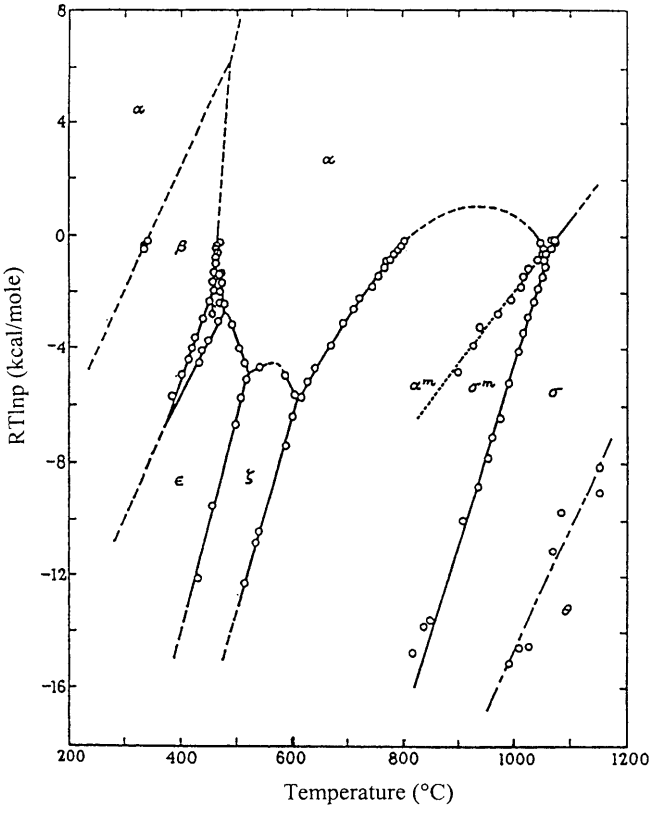

Fig. 2 Ranges of oxygen pressure in which various phases are stable as a function of temperature [3]

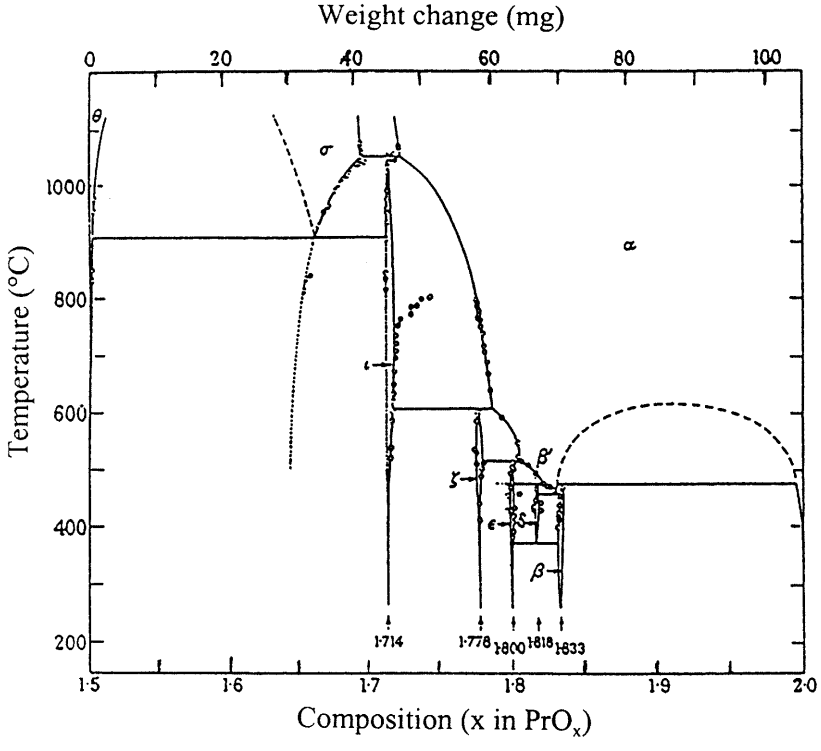

Fig. 1 Projection of the phase diagram of the praseodymium-oxygen system on the temperature-composition plane [3]

the beta phase is not stable, as can be seen from Fig. 2.

Experimental

Powdered Pr_6O_{11} (99.9% purity) was purchased from ChemPur Chemical (Karlsruhe, Germany). It was made into a cylinder about 9 mm diameter and 30 mm long by isostatically pressing at 38 kN/cm^2. The cylinder was sintered in air at 1000 °C for 24 h, cooled to room temperature and annealed in air at 350 °C for an additional 24 h. This treatment resulted in the expulsion of any water that might have been initially present in the crystal structure. The annealed sample cylinder was cut into small coin-shaped pellets (9 mm in diameter and about 2 mm thick), suitable for electrical measurements, by use of a diamond saw.

Powder X-ray diffraction measurements were carried out on several samples to monitor the crystal structure using a Seifert Model 3000 X-ray diffractometer with Cu Kα radiation.

Unfortunately, the phase changes that occur as samples are cooled from the sintering temperature cause the formation of many small cracks. Thus it is not possible to prevent the transport of gaseous oxygen to and from the two electrolyte/electrode interfaces.

The frequency dependence of the complex impedance was measured over the frequency range 100 Hz to 13 MHz using a Hewlett-Packard model 4192A impedance bridge. Experiments were conducted in the temperature range 75–400 °C in gas environments with different values of oxygen partial pressure: oxygen, air, 1000 ppm oxygen in argon, and 2 ppm oxygen in argon. Some DC conductivity measurements were also made in both an air and a low oxygen activity environment. The phase equilibrium data in Fig. 2 indicate that the samples that are measured in air in this temperature range have the beta phase, whereas those measured in partial pressures of either 2 ppm or 1000 ppm oxygen have the epsilon phase.

Platinum paste electrodes were applied to the opposite sides of the sample. In order to achieve equilibrium conditions, the sample was equilibrated at constant temperature for 1–2 h prior to each impedance measurement.

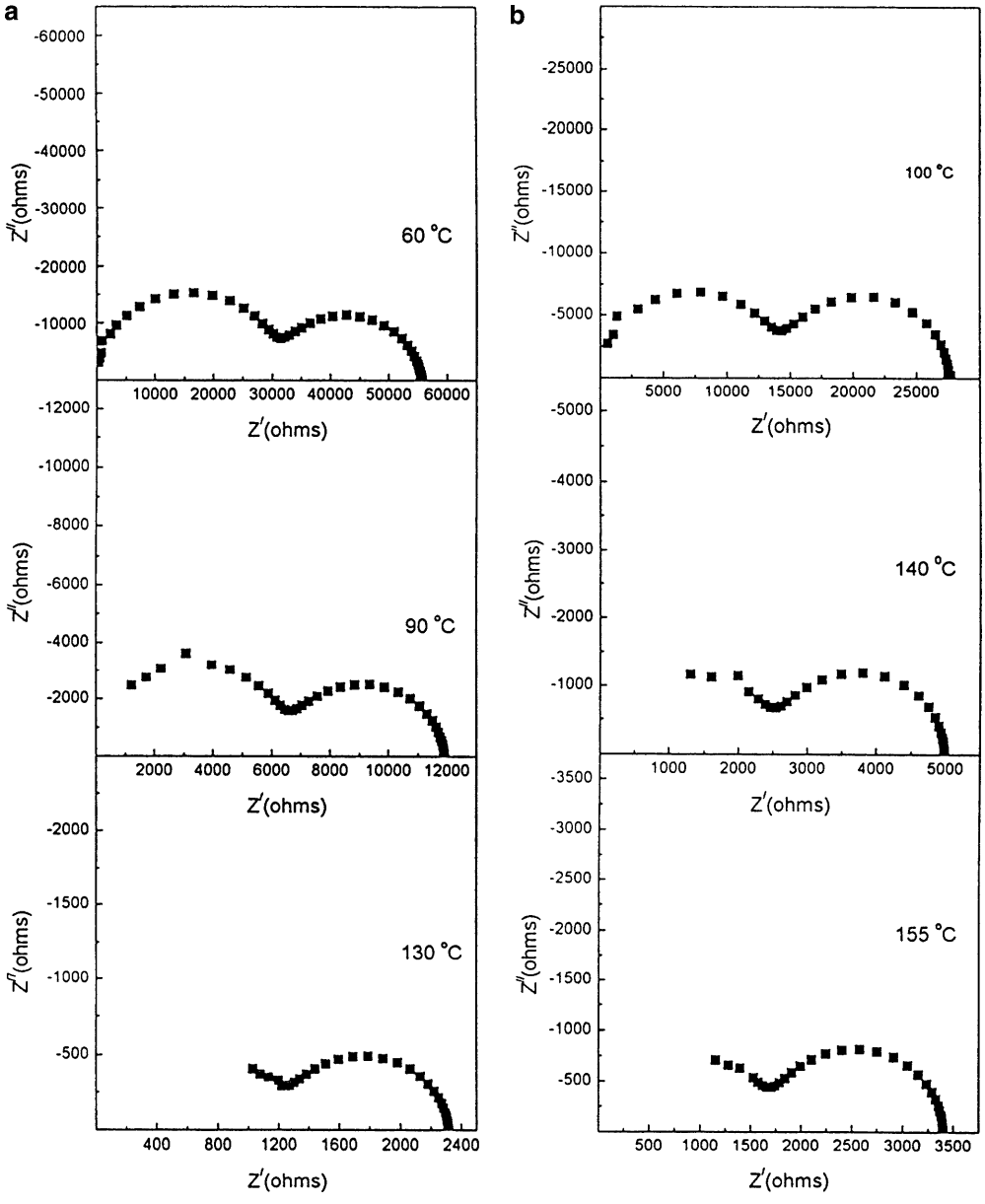

Fig. 3 Typical results of complex impedance measurements: **a** measurements in air; **b** measurements in 2 ppm oxygen

Results and discussion

Typical results of the complex impedance measurements are shown in Fig. 3. It can be seen that measurements in both air and 2 ppm oxygen produced two distinct semicircles, but with no visible low-frequency tails. The lack of a low-frequency capacitive tail indicates that

Table 2 Observed values of capacity

Phase	Temperature (°C)	High-frequency semicircle (pF)	Low-frequency semicircle (nF)
Beta	60	4.3	0.28
Beta	90	3.8	0.31
Epsilon	100	5.0	0.34

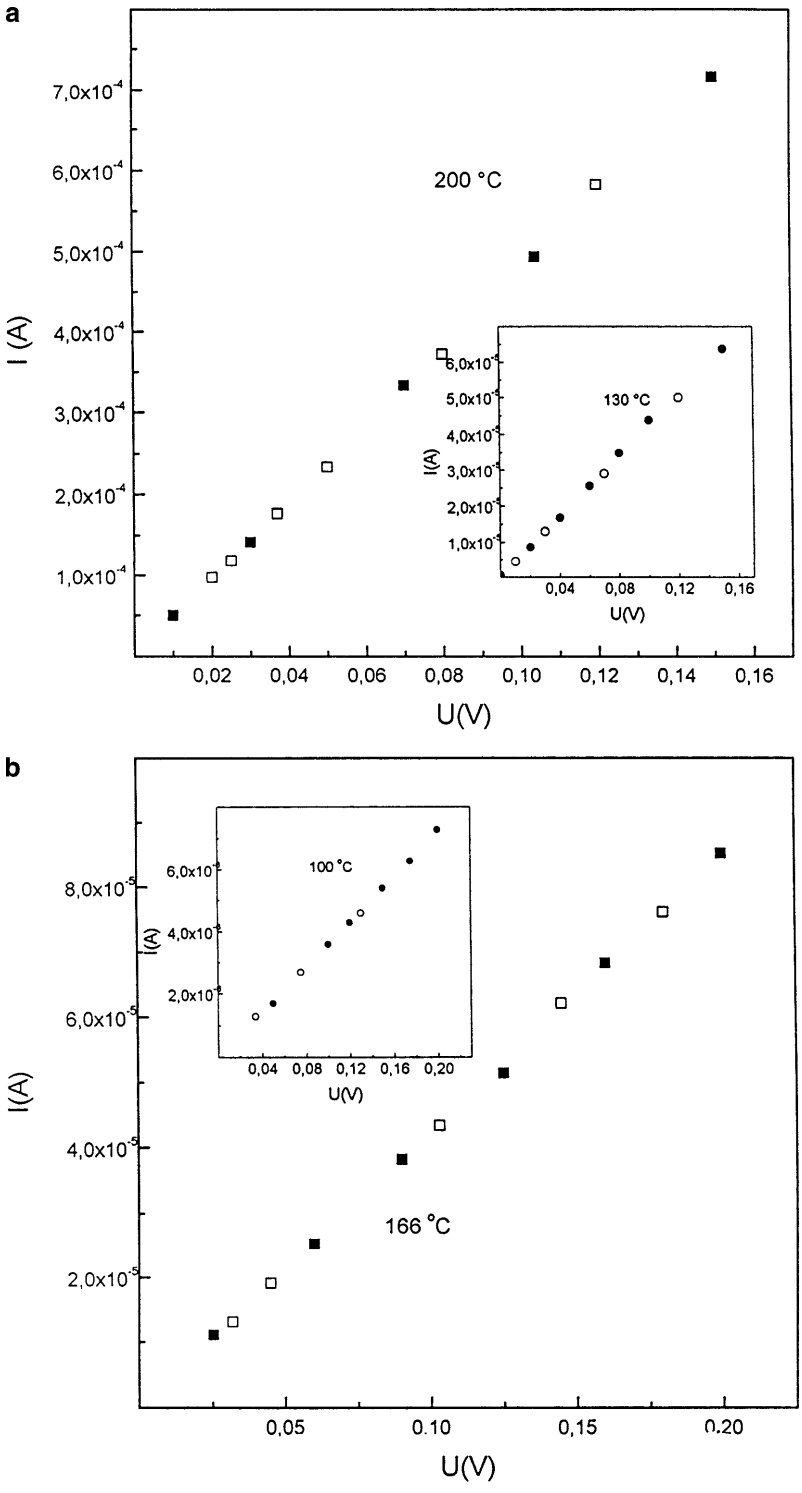

Fig. 4 Results of DC measurements **a** in air and **b** in 2 ppm oxygen. *Filled points* were from measurements upon raising the voltage, and *open points* when the voltage was lowered

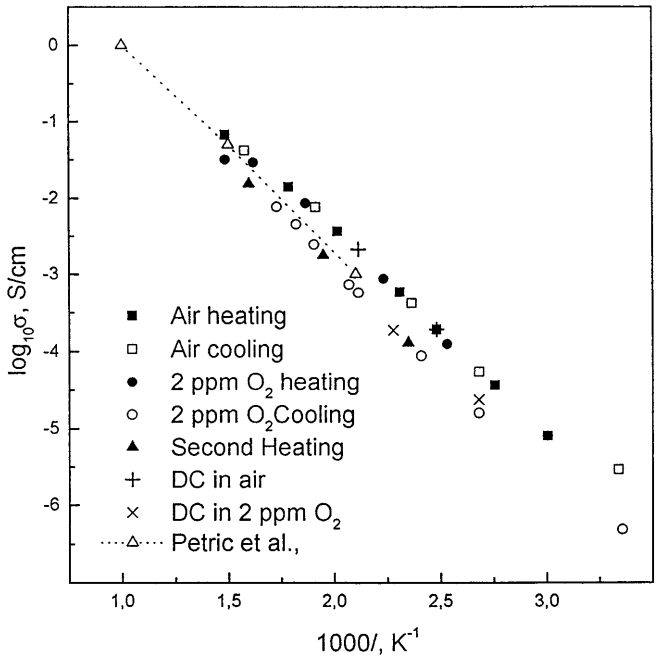

Fig. 5 Temperature dependence of the conductivity for two different values of oxygen partial pressure, as determined from complex impedance measurements. The *upper curve* shows data measured in air. Data along the *lower curve* were measured in 2 ppm oxygen. Points representing the results of DC measurements in air and 2 ppm oxygen are also included, as well as results from [10]

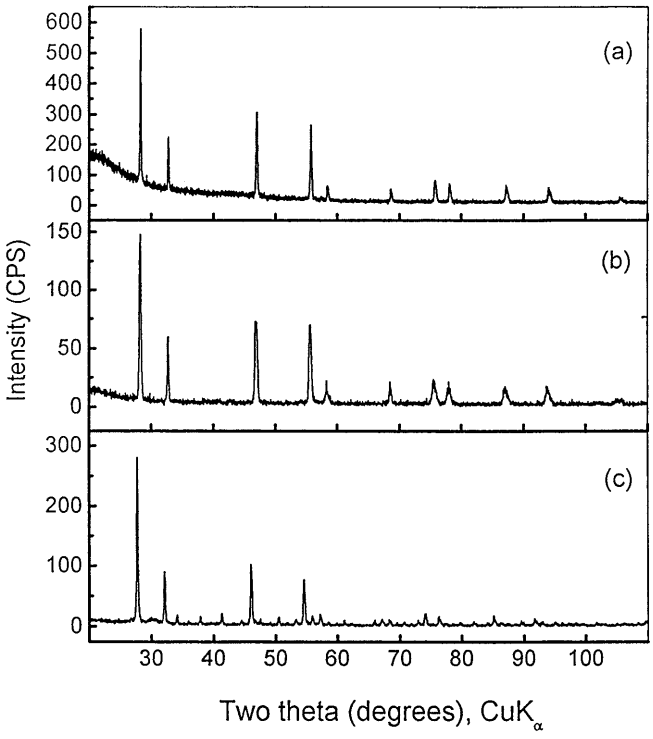

Fig. 6 Powder X-ray diffraction spectra taken at ambient temperature after performing experiments: **a** annealed in air overnight at 400 °C; **b** after conductivity measurements in 2 ppm oxygen; **c** after conductivity measurements in hydrogen

the electrolyte/electrode interfaces were not blocking to the charge-carrying species. This could be due to the presence of some electronic conductivity. It could also indicate that the electrodes were not completely blocking to ions under the experimental conditions employed. The fact that the samples contained cracks allowed both good access to the surrounding gas as well as transport of gaseous oxygen between the electrodes. Thus the platinum paste electrodes could not be considered to be completely blocking to ions.

If the charge transport were entirely due to electronic species, the two semicircles would not be present at the higher frequencies. This indicates that at least a portion of the charge transport is carried by ionic species.

The capacity values were evaluated from the experimental parameters at the top of the semicircles. For a simple parallel *R-C* combination the frequency, resistance and capacity are related at that location by:

$$2\pi fRC = 1 \tag{1}$$

where f is the AC frequency. Taking into account the resistance at the top of the semicircles, one can determine the relevant capacity values. The results are shown in Table 2. The lower values are in the general range expected for a simple parallel-plate geometrical configuration of the electrodes across a material that is not a good electronic conductor. The fact that a second semicircle was observed indicates that another mechanism was also present. Its time constant is greater, indicating that the product of the corresponding resistance and its parallel capacitance is larger than in the case of the first mechanism. From the existing information it is not clear whether this is due to a grain boundary effect or is related to the presence of the cracks.

Data on the electrical conductivity, the reciprocal of the total resistivity, were obtained from the

Table 3 Data for a number of mixed-conducting oxides

Material	σ(60 °C) (S/cm)	σ(850 °C) (S/cm)	E_a (eV/atom)	Ref
$La_{0.9}Sr_{0.1}Ga_{0.72}Fe_{0.08}Mg_{0.20}O_{3-d}$	$<10^{-10}$	0.10	0.58	[11]
$La_{0.9}Sr_{0.1}Ga_{0.72}Co_{0.08}Mg_{0.20}O_{3-d}$	$<10^{-10}$	0.10	0.43	[11]
$La_{0.9}Ga_{0.75}Mg_{0.22}Nb_{0.03}O_{3-d}$	4.9×10^{-9}	0.041	0.77	[12]
$La_{0.9}Ga_{0.65}Mg_{0.28}$ $Nb_{0.07}O_{3-d}$	5.0×10^{-9}	0.041	0.77	[12]
$Pr_{0.97}Ca_{0.07}Ga_{0.85}Mg_{0.15}O_{3-d}$	–	0.07	0.65	[13]
$Pr_{0.97}Sr_{0.07}Ga_{0.85}Mg_{0.15}O_{3-d}$	$<10^{-10}$	0.10	0.88	[13]
Pr_6O_{11}	7.6×10^{-6}	1.40	0.52	Present study

low-frequency intercept on the real (Z') axis of the complex impedance plots. DC experiments were also performed at several temperatures, and gave linear I/V curves, as illustrated in Fig. 4.

The temperature dependence of the conductivity was measured over the temperature range 75–400 °C. The results are shown in Fig. 5. Only data for samples held in air and in 2 ppm oxygen are included. It can be seen that the results fall upon two almost-parallel curves. Values taken at a series of increasing temperatures corresponded well with those taken upon decreasing the temperature. Likewise, cycling back and forth between air and the low oxygen partial pressure consistently shifted the data between the two curves. It can be seen that the AC and DC experiments gave equivalent results, as expected from the shape of the complex impedance data. The results of experiments in an atmosphere of 1000 ppm oxygen were essentially the same as those with 2 ppm oxygen. The epsilon phase was present in both cases, as seen from the phase equilibria data in Fig. 2.

The activation energies for the electrical conduction in the beta and epsilon phases were evaluated from the respective temperature dependences. They were found to be essentially the same, about 0.52 eV/atom for the beta phase samples measured in air, and about 0.51 eV/atom for the epsilon phase at the lower oxygen partial pressures. It is interesting that these are comparable to the values of the activation energies for charge transport in a number of the lower temperature mixed-conducting oxides. This is shown in Table 3.

Experiments were also undertaken to measure the electrical conductivity in a hydrogen atmosphere. Under these conditions the iota phase is stable. The conductivity of this phase was so low that it could not be measured with the HP instrument, even up to 600 °C.

Powder X-ray diffraction measurements were made at ambient temperature of samples that had been measured in air, at the low oxygen partial pressure atmosphere, and in hydrogen. The results are shown in Fig. 6. It is clear that the basic "mother" fluorite structure is retained in all cases. The lattice parameter values were consistent with the more extensive measurements reported [5] when the influence of the atmosphere upon the stability of the different phases, illustrated in Fig. 2, is taken into account.

It was also noticed that the color of the sample changed during the experiments in the hydrogen atmosphere. The low oxygen content iota phase has a darker appearance than either of the other two phases investigated.

Conclusions

Experimental results have been presented on the electrical transport behavior in materials in the PrO_x system. They contain extended defects, in which stoichiometric variations are accommodated by changes in the topotactically ordered arrangements of large localized concentrations of oxide ion vacancies that divide the structure up into microdomains. They have essentially no isolated point defects. This is quite different from the conventional model of a solid solution, in which compositional changes and mass and charge transport occur by the motion of randomly distributed ionic and electronic point defects.

It was shown that the beta phase in the praseodymium oxide system, Pr_6O_{11}, exhibits quite high values of electrical conduction at modest temperatures. The conductivity is about a factor of three lower under conditions in which the epsilon phase is stable, and much lower when the iota phase is present.

The presence of the semicircles in the complex impedance plots, as well as the magnitude of the geometric capacitance, indicate that ionic transport becomes important in the measurements made at higher frequencies. Under DC conditions, when the ionic transport is blocked, electronic transport is dominant. This is what is expected for a mixed conductor.

Some experiments were undertaken using galvanic cell techniques to determine the ionic and electronic transference numbers. Although there were transient indications of a cell voltage when two-phase combinations with different oxygen activities were used as the electrodes, no reliable data could be obtained. There are two possible explanations for the failure of those experiments. One is the difficulty in achieving equilibria in the electrodes at the low temperatures. Another is the presence of cracks due to the volume changes accompanying the phase transformations as the

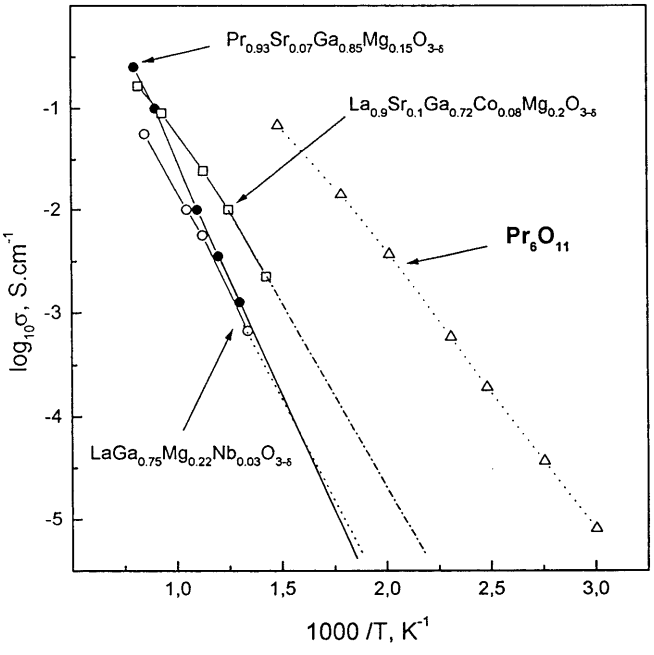

Fig. 7 Comparison of the temperature dependence of the conductivity of beta PrO_x with values reported for several LSGM-related mixed-conducting oxides

temperature and oxygen pressure were changed that could allow chemical short-circuit transport between the electrodes.

The electrical conductivity of these materials is significantly higher that that reported for some of the LSGM-related mixed-conducting oxides investigated recently, as shown in Fig. 7. The (partially extrapolated) conductivities and activation energies are compared in Table 3.

References

1. Eyring L, O'Keeffe M (1970) The chemistry of extended defects in non-metallic solids. North-Holland, Amsterdam
2. Kosuge K (1994) Chemistry of non-stoichiometric compounds. Oxford University Press, Oxford
3. Hyde BG, Bevan DJM, Eyring L (1966) Philos Trans R Soc London Ser A 259:583
4. Lott U (1968) PhD Thesis, University of Karlsruhe
5. Burnham DA, Eyring L (1968) J Phys Chem 72:4415
6. Kordis J, Eyring L (1968) J Phys Chem 72:2044
7. Stotz S, Wagner C (1966) Ber Bunsenges Phys Chem 70:781
8. Wagner C (1968) Ber Bunsenges Phys Chem 72:778
9. Netz A, Chu WF, Thangadurai V, Huggins RA, Weppner W (1999) Ionics 5:426
10. Huang P, Petric A, Gong W (1997) Electrochem Soc Proc 97-24:396
11. Ullmann H, Trofimenko N (1999) Solid State Ionics 119:1
12. Kharton VV, Yaremchenko AA, Viskup AP, Nather GC, Naumovich EN, Marques FMB (2000) Solid State Ionics 128:79
13. Ishihara T, Furutani H, Arikawa H, Honda M, Akbay T, Takita Y (1999) J Electrochem Soc 146:1643